Electronic Supplementary Information

Probe molecular diffusivity in single ternary inorganic-organic microdroplets via interface ozonolysis of thiosulfate

Tzu-Chiao Hung,[a] Feng-Yu Lin,[a] Shao-Hung Hsu,[a] Toshio Kasai[a,b] and Yuan-Pin Chang,*[a,c]

[a]Department of Chemistry, National Sun Yat-sen University, Kaohsiung 80424, Taiwan

[b] Division of Precision Engineering and Applied Physics, Graduate School of Engineering, Osaka University, Suita, Osaka Japan

[c]Aerosol Science Research Center, National Sun Yat-sen University, Kaohsiung 80424, Taiwan

[1]To whom correspondence may be addressed. Email: ypchang@mail.nsysu.edu.tw

I. Experimental conditions

Table S1. Experimental conditions of all reaction kinetic measurements for ternary mixtures of aqueous sodium thiosulfate (T) and sucrose (S), labelled with their stoichiometric ratios "5T1S", "4T2S", "3T3S" and "2T4S" in the "Type" column. The "*X*T*Y*S" label means its mass ratio of STS : sucrose : water is *X* : *Y* : 15. *P*: pressure of gaseous ozone pressure; RH: relative humidity; *r*: radius; *I*: ionic strength; $[STS]_0$: initial concentration of sodium thiosulfate before reaction in each microdroplet; $[SUC]_0$: concentration of sucrose in each microdroplet.

Expt. #	Type	*P* / ppm	RH / %	$[STS]_0$ / M	$[SUC]_0$ / M	*r* / µm	*I* / M
1	5T1S	13.7	91.0	2.1	0.2	2.6	6.17
2*	5T1S	16.9	82.6	2.8	0.2	3.5	8.50
3	5T1S	16.2	83.6	2.0	0.2	3.4	6.12
4	5T1S	13.9	68.0	4.1	0.5	3.0	12.4
5	5T1S	14.1	65.7	3.6	0.4	3.2	10.7
6	5T1S	16.1	60.7	4.0	0.6	3.1	11.9
7	5T1S	16.6	47.4	8.6	0.9	2.7	25.7
8*	5T1S	15.8	40.0	5.4	0.9	3.1	16.2
9	5T1S	14.1	38.6	5.2	0.5	2.8	15.5
10*	5T1S	12.7	31.3	7.6	1.2	3.1	22.7
11	5T1S	15.0	21.3	9.0	1.5	3.2	27.0
12*	5T1S	15.8	21.1	14.2	1.9	2.8	42.6
13	4T2S	15.0	94.7	0.7	0.2	4.3	2.05
14*	4T2S	14.8	88.7	2.7	0.3	2.8	8.18
15	4T2S	15.1	84.4	1.2	0.4	3.1	3.54
16	4T2S	13.9	58.9	4.7	1.1	3.4	14.2
17	4T2S	14.1	58.9	4.5	1.1	2.8	14.0
18	4T2S	13.9	58.8	4.5	1.2	3.1	13.4
19	4T2S	13.1	55.5	4.8	1.1	2.8	14.5
20	4T2S	19.5	47.6	5.0	1.3	3.0	15.0
21	4T2S	13.9	45.1	5.6	1.4	2.8	13.4
22	4T2S	14.4	43.9	6.3	1.5	3.2	18.8
23	4T2S	15.6	42.6	6.4	1.6	2.6	19.2

24*	4T2S	19.4	42.1	6.2	1.6	2.7	18.7
25	4T2S	14.4	35.4	7.2	1.9	2.8	21.4
26	4T2S	14.9	34.1	6.5	2.1	3.0	19.6
27*	4T2S	13.3	33.3	7.0	2.8	2.7	20.8
28	4T2S	14.7	33.0	6.5	2.2	3.1	19.5
29*	4T2S	13.4	27.4	7.6	2.6	3.1	22.8
30	4T2S	14.0	25.6	7.9	2.4	2.7	25.6
31	4T2S	16.4	21.6	9.7	2.9	2.4	29.2
32*	3T3S	12.7	84.0	2.4	1.6	3.7	7.06
33	3T3S	11.8	60.0	3.6	2.3	4.1	10.8
34*	3T3S	13.5	58.3	3.4	2.3	3.3	10.1
35	3T3S	12.0	39.7	4.1	2.9	3.0	12.3
36*	3T3S	12.5	39.3	4.1	2.9	3.0	12.2
37	3T3S	13.9	23.0	5.5	3.6	2.8	16.6
38*	3T3S	13.1	22.3	5.0	3.4	3.4	14.9
39*	2T4S	11.7	88.7	1.1	1.8	3.4	3.43
40	2T4S	11.5	87.1	1.4	2.2	3.2	4.26
41	2T4S	12.1	86.1	1.1	1.8	4.1	3.21
42	2T4S	1.2	83.0	1.2	2.0	3.9	3.70
43*	2T4S	13.7	49.2	1.8	3.1	3.6	5.43
44*	2T4S	15.7	37.5	2.5	4.0	2.6	7.38
45	2T4S	15.5	36.8	2.4	4.2	3.5	7.07

Table S2. Experimental conditions of all reaction kinetic measurements for ternary mixtures of aqueous sodium thiosulfate (T) and glucose (G), labelled with their stoichiometric ratios "5T1G", "4T2G", "3T3G" and "2T4G" in the "Type" column. The "*X*T*Y*G" label means its mass ratio of STS : glucose : water is *X* : *Y* : 15. *P*: pressure of gaseous ozone pressure; RH: relative humidity; *r*: radius; *I*: ionic strength; $[STS]_0$: initial concentration of sodium thiosulfate before reaction in each microdroplet; $[GLU]_0$: concentration of glucose in each microdroplet.

Expt. #	Type	*P* / ppm	RH / %	$[STS]_0$ / M	$[GLU]_0$ / M	*r* / µm	*I* / M
46	5T1G	14.3	96.2	2.4	0.7	4.6	7.25
47	5T1G	8.04	32.8	7.2	1.5	2.9	21.6
48	5T1G	11.1	26.3	8.8	1.9	2.9	26.4
49	5T1G	13.3	23.0	11.2	2.0	3.1	33.6
50	5T1G	9.61	18.0	10.4	1.8	3.0	31.1
51	5T1G	7.59	17.5	10.2	1.8	2.8	30.6
52	4T2G	15.2	97.8	4.5	1.4	3.7	13.5
53	4T2G	15.3	37.6	8.3	3.9	3.1	24.8
54	4T2G	15.2	35.5	8.1	3.5	2.8	24.2
55	4T2G	17.9	28.2	10.0	5.1	3.1	30.0
56	4T2G	13.9	27.7	9.7	6.2	2.8	29.1
57	4T2G	14.6	22.0	12.8	7.7	3.0	38.5
58	4T2G	18.9	19.2	10.5	4.5	2.6	31.5
59	3T3G	9.1	89.9	3.4	2.0	3.4	7.37
60	3T3G	11.1	28.9	6.1	4.1	3.1	5.96
61	3T3G	11.1	28.4	7.0	5.1	3.3	10.8
62	3T3G	13.8	24.4	7.4	5.5	3.2	10.1
63	3T3G	11.8	22.6	7.9	4.4	3.1	14.9
64	2T4G	15.3	93.5	1.9	3.0	4.4	5.92
65	2T4G	11.1	34.6	3.8	7.4	3.0	11.3
66	2T4G	14.8	28.6	4.1	7.7	3.1	12.4
67	2T4G	15.2	28.1	3.8	7.4	3.1	11.3
68	2T4G	12.1	20.7	3.8	7.1	3.0	11.3
69	2T4G	15.5	20.5	3.7	7.4	3.4	11.2

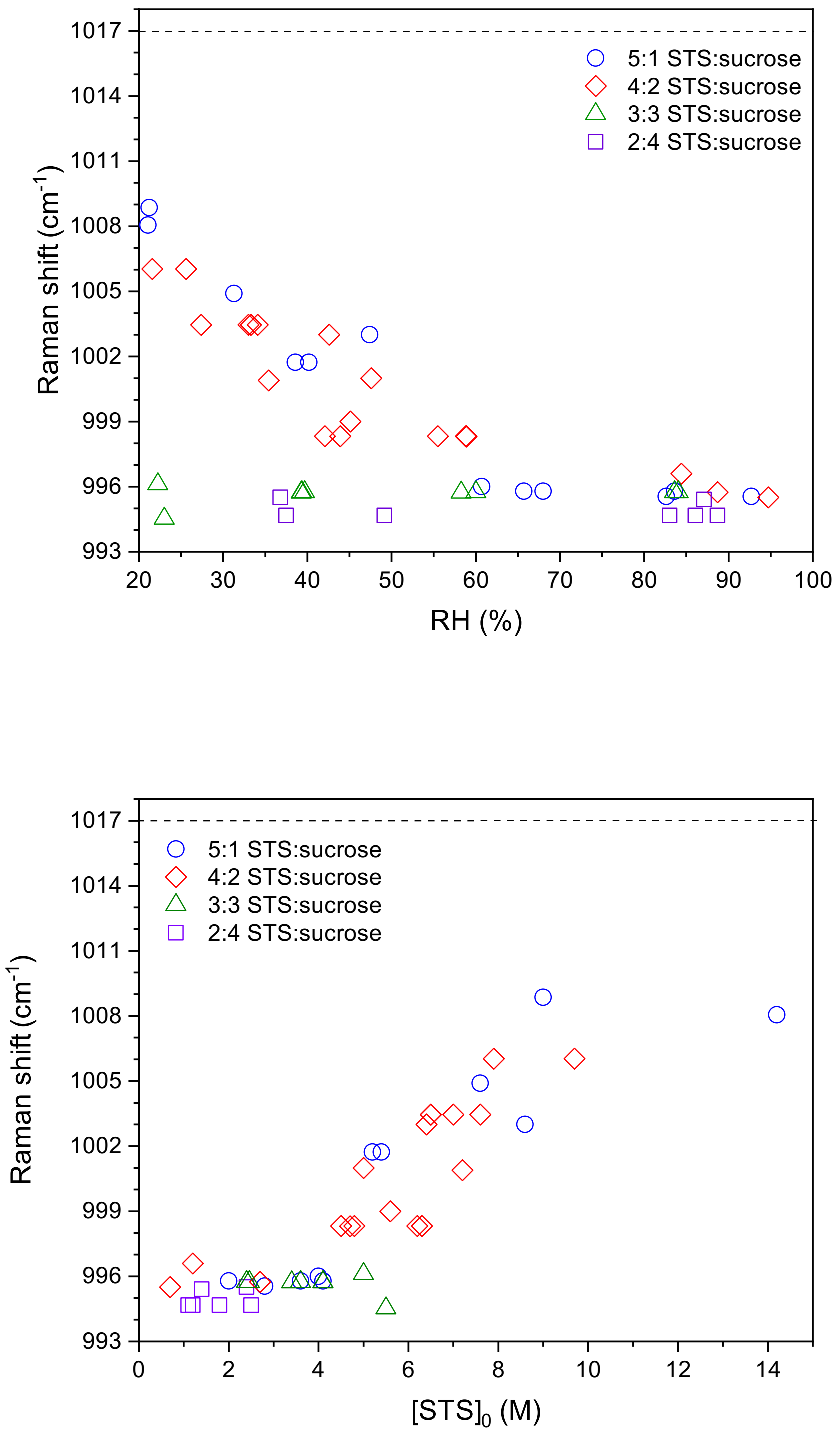

Fig. S1 Raman shifts of the $\nu_{sym(S-O)}$ band of $S_2O_3^{2-}$(aq) observed in single microdroplets under different RH and mass ratios of STS and sucrose (top) versus RH and (bottom) versus $[STS]_0$. Dash line: Raman shifts of this band in solid phase. Note that the spectral resolution is around 7 cm^{-1}.

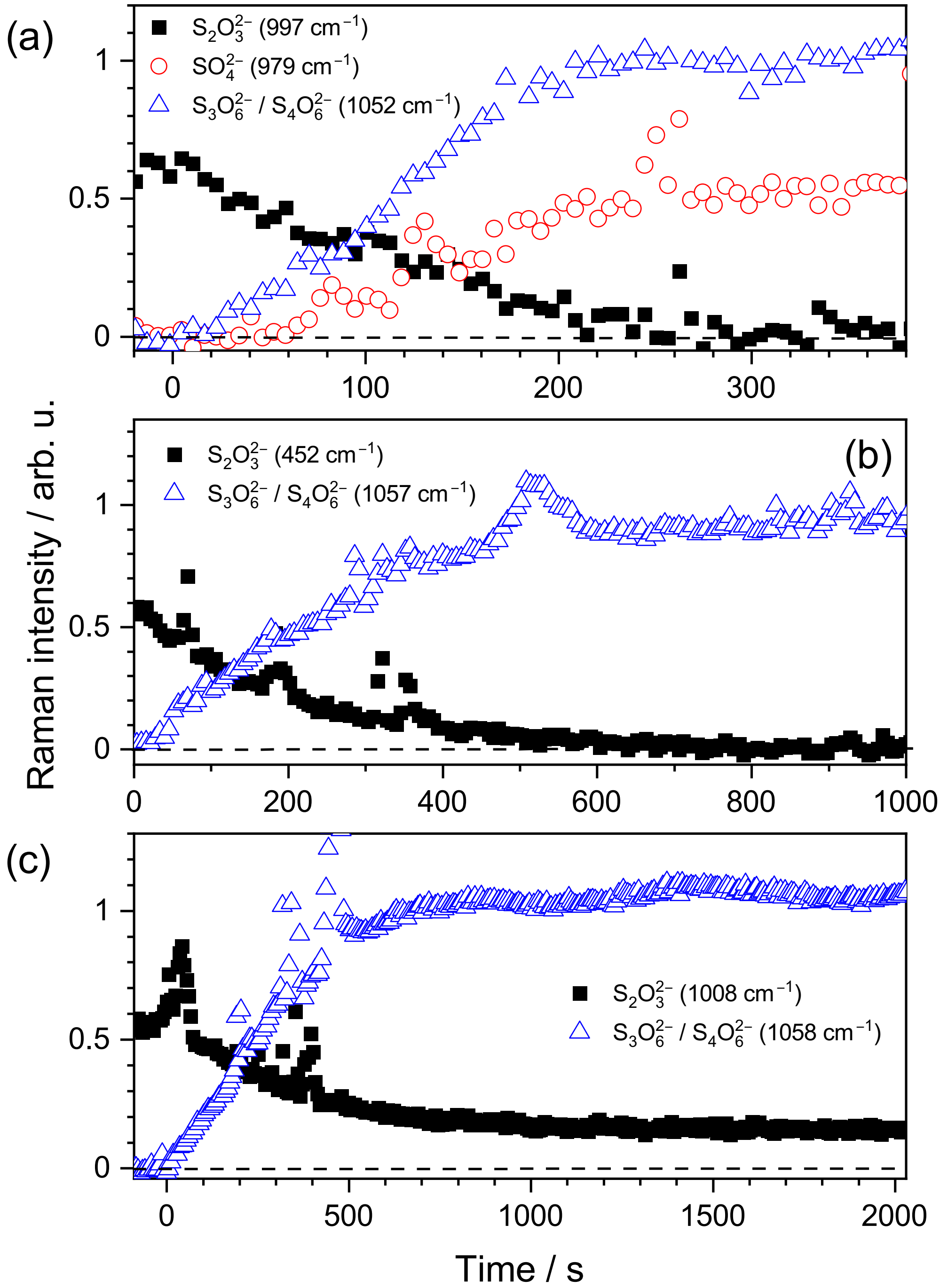

Fig. S2 Representative time profiles of integrated Raman intensities assigned to reactant $S_2O_3^{2-}$ (solid squares) and products SO_4^{2-} (hollow circles) and $S_3O_6^{2-}/S_4O_6^{2-}$ (hollow triangles) for (a) Expt. 02 (STS:sucrose in 5:1 mass ratio at 83% RH), (b) Expt. 24 (STS:sucrose in 4:2 mass ratio at 42% RH) and (c) Expt. 10 (STS:sucrose in 5:1 mass ratio at 31% RH).

II. Input parameters of KM-SUB model simulations

Table S3. Input parameters of KM-SUB simulations via Scenario 1 for the data of Expt. # listed below.

Expt. #	1 / 5T1S	2 / 5T1S	3 / 5T1S	4 / 5T1S	5 / 5T1S	6 / 5T1S
$D_{b,O}$	1.6×10^{-6}	8.0×10^{-6}	1.6×10^{-6}	8.0×10^{-10}	2.9×10^{-10}	9.6×10^{-11}
$D_{b,T}$	1.0×10^{-6}	5.0×10^{-6}	1.0×10^{-6}	5.0×10^{-10}	1.8×10^{-10}	6.0×10^{-11}
k_{SLR}	1.9×10^{-10}	2.1×10^{-10}	1.9×10^{-10}	2.5×10^{-10}	2.2×10^{-10}	2.4×10^{-10}
$[O_3]_g$	3.7×10^{14}	4.5×10^{14}	4.4×10^{14}	3.7×10^{14}	5.5×10^{14}	4.3×10^{14}
$[STS]_{b,0}$	1.2×10^{21}	1.7×10^{21}	1.2×10^{21}	2.5×10^{21}	2.5×10^{21}	2.4×10^{21}
$K_{sol,O3}$	2.3×10^{-6}	1.2×10^{-6}	2.4×10^{-6}	4.0×10^{-7}	3.6×10^{-7}	4.3×10^{-7}
r_p	2.58	3.51	3.38	3.01	3.00	3.14
Expt. #	7 / 5T1S	8 / 5T1S	9 / 5T1S	11 / 5T1S	12 / 5T1S	13 / 4T2S
$D_{b,O}$	1.1×10^{-10}	5.3×10^{-11}	5.8×10^{-11}	1.6×10^{-13}	4.8×10^{-15}	5.8×10^{-7}
$D_{b,T}$	6.6×10^{-11}	3.3×10^{-11}	3.6×10^{-11}	$< 1.0 \times 10^{-13}$	$< 3.0 \times 10^{-15}$	3.6×10^{-7}
k_{SLR}	4.6×10^{-10}	3.0×10^{-10}	2.9×10^{-10}	4.9×10^{-10}	9.9×10^{-10}	5.5×10^{-11}
$[O_3]_g$	4.5×10^{14}	4.3×10^{14}	3.8×10^{14}	4.0×10^{14}	4.2×10^{14}	4.0×10^{14}
$[STS]_{b,0}$	5.2×10^{21}	3.3×10^{21}	3.1×10^{21}	5.3×10^{21}	8.5×10^{21}	4.1×10^{20}
$K_{sol,O3}$	9.6×10^{-9}	1.2×10^{-7}	1.7×10^{-7}	5.4×10^{-9}	7.5×10^{-11}	6.8×10^{-6}
r_p	2.71	3.10	2.77	3.20	3.94	4.30
Expt. #	14 / 4T2S	15 / 4T2S	16 / 4T2S	17 / 4T2S	18 / 4T2S	19 / 4T2S
$D_{b,O}$	1.4×10^{-6}	2.2×10^{-6}	1.0×10^{-10}	3.2×10^{-11}	1.3×10^{-10}	4.8×10^{-10}
$D_{b,T}$	1.9×10^{-5}	1.4×10^{-6}	6.4×10^{-11}	2.0×10^{-11}	8.2×10^{-11}	3.0×10^{-10}
k_{SLR}	2.0×10^{-10}	1.7×10^{-10}	2.7×10^{-10}	2.7×10^{-10}	2.6×10^{-10}	2.7×10^{-10}
$[O_3]_g$	4.0×10^{14}	4.0×10^{14}	3.7×10^{14}	3.8×10^{14}	3.8×10^{14}	3.5×10^{14}
$[STS]_{b,0}$	1.6×10^{21}	7.1×10^{20}	2.9×10^{21}	2.8×10^{21}	2.7×10^{21}	2.9×10^{21}
$K_{sol,O3}$	1.3×10^{-6}	4.3×10^{-6}	1.9×10^{-7}	1.9×10^{-7}	2.2×10^{-7}	1.7×10^{-7}
r_p	2.83	3.07	3.44	2.83	3.08	2.83
Expt. #	20 / 4T2S	21 / 4T2S	22 / 4T2S	23 / 4T2S	24 / 4T2S	25 / 4T2S
$D_{b,O}$	2.4×10^{-10}	5.6×10^{-11}	6.2×10^{-11}	2.1×10^{-11}	8.8×10^{-11}	5.6×10^{-11}
$D_{b,T}$	1.5×10^{-10}	3.5×10^{-11}	3.9×10^{-11}	1.3×10^{-11}	5.5×10^{-11}	3.5×10^{-11}
k_{SLR}	2.8×10^{-10}	3.2×10^{-10}	3.3×10^{-10}	3.4×10^{-10}	3.3×10^{-10}	3.8×10^{-10}
$[O_3]_g$	5.2×10^{14}	4.0×10^{14}	3.9×10^{14}	4.2×10^{14}	5.2×10^{14}	3.8×10^{14}
$[STS]_{b,0}$	3.0×10^{21}	3.4×10^{21}	3.8×10^{21}	3.9×10^{21}	3.8×10^{21}	4.3×10^{21}
$K_{sol,O3}$	1.4×10^{-7}	8.3×10^{-8}	4.8×10^{-8}	4.0×10^{-8}	4.5×10^{-8}	1.9×10^{-8}

r_p	2.95	2.83	3.20	2.58	2.71	2.83
Expt. #	31 / 4T2S	32 / 3T3S	33 / 3T3S	34 / 3T3S	37 / 3T3S	38 / 3T3S
$D_{b,O}$	6.7×10^{-13}	3.7×10^{-7}	6.6×10^{-10}	4.0×10^{-10}	1.3×10^{-13}	1.6×10^{-14}
$D_{b,T}$	4.2×10^{-13}	2.3×10^{-7}	4.1×10^{-10}	2.5×10^{-10}	8.0×10^{-14}	1.0×10^{-14}
k_{SLR}	5.4×10^{-10}	1.9×10^{-10}	2.3×10^{-10}	2.2×10^{-10}	3.0×10^{-10}	2.8×10^{-10}
$[O_3]_g$	4.4×10^{14}	3.4×10^{14}	3.2×10^{14}	3.6×10^{14}	3.8×10^{14}	3.5×10^{14}
$[STS]_{b,0}$	5.9×10^{21}	1.4×10^{21}	2.2×10^{21}	2.0×10^{21}	3.3×10^{21}	3.0×10^{21}
$K_{sol,O3}$	1.6×10^{-9}	9.9×10^{-7}	2.6×10^{-7}	3.1×10^{-7}	3.1×10^{-8}	5.5×10^{-8}
r_p	2.44	3.69	4.06	3.32	2.78	39 / 3T3S
Expt. #	39 / 2T4S	40 / 2T4S	41 / 2T4S	42 / 2T4S	43 / 2T4S	44 / 4T2S
$D_{b,O}$	3.5×10^{-6}	1.6×10^{-5}	2.0×10^{-5}	3.2×10^{-6}	1.1×10^{-10}	9.6×10^{-14}
$D_{b,T}$	2.2×10^{-6}	1.0×10^{-5}	1.2×10^{-5}	2.0×10^{-6}	6.9×10^{-11}	$< 6.0 \times 10^{-14}$
k_{SLR}	1.7×10^{-10}	1.7×10^{-10}	1.6×10^{-10}	1.6×10^{-10}	1.8×10^{-10}	2.0×10^{-10}
$[O_3]_g$	3.1×10^{14}	3.1×10^{14}	3.3×10^{14}	3.2×10^{13}	3.7×10^{14}	4.2×10^{14}
$[STS]_{b,0}$	6.9×10^{20}	8.6×10^{20}	6.4×10^{20}	7.4×10^{20}	1.1×10^{21}	1.5×10^{21}
$K_{sol,O3}$	2.3×10^{-6}	1.6×10^{-6}	2.5×10^{-6}	2.0×10^{-6}	7.3×10^{-7}	2.9×10^{-7}
r_p	3.44	3.18	4.06	3.87	3.57	3.57
Expt. #	45 / 4T2S	46 / 5T1G	47 / 5T1G	50 / 5T1G	51 / 5T1G	52 / 4T2G
$D_{b,O}$	1.1×10^{-12}	1.1×10^{-5}	3.7×10^{-11}	1.6×10^{-15}	9.8×10^{-15}	1.3×10^{-5}
$D_{b,T}$	< 7.1	6.9×10^{-6}	2.3×10^{-11}	$< 1.0 \times 10^{-15}$	$< 6.1 \times 10^{-15}$	8.0×10^{-6}
k_{SLR}	1.9×10^{-10}	2.0×10^{-10}	3.8×10^{-10}	5.9×10^{-10}	5.7×10^{-10}	2.6×10^{-10}
$[O_3]_g$	4.2×10^{14}	3.9×10^{14}	2.2×10^{14}	2.6×10^{14}	2.0×10^{14}	4.1×10^{14}
$[STS]_{b,0}$	1.4×10^{21}	1.5×10^{21}	4.3×10^{21}	6.2×10^{21}	5.8×10^{21}	2.7×10^{21}
$K_{sol,O3}$	2.0×10^{-6}	1.4×10^{-6}	2.2×10^{-8}	1.6×10^{-9}	1.8×10^{-9}	2.0×10^{-7}
r_p	3.52	4.59	2.89	3.01	2.83	3.69
Expt. #	53 / 4T2G	54 / 4T2G	57 / 4T2G	58 / 4T2G	59 / 3T3G	62 / 3T3G
$D_{b,O}$	3.7×10^{-11}	1.1×10^{-10}	3.2×10^{-14}	9.6×10^{-11}	2.2×10^{-5}	1.3×10^{-14}
$D_{b,T}$	2.3×10^{-11}	7.0×10^{-11}	$< 2.0 \times 10^{-14}$	$< 3.0 \times 10^{-15}$	1.4×10^{-5}	$< 8.0 \times 10^{-15}$
k_{SLR}	4.4×10^{-10}	4.3×10^{-10}	8.2×10^{-10}	6.0×10^{-10}	2.2×10^{-10}	3.9×10^{-10}
$[O_3]_g$	4.1×10^{14}	4.1×10^{14}	3.9×10^{14}	5.1×10^{14}	2.5×10^{14}	3.7×10^{14}
$[STS]_{b,0}$	5.0×10^{21}	4.9×10^{21}	7.7×10^{21}	6.3×10^{21}	2.0×10^{21}	4.5×10^{21}
$K_{sol,O3}$	3.2×10^{-9}	4.4×10^{-9}	1.5×10^{-11}	4.0×10^{-10}	3.7×10^{-7}	2.9×10^{-9}
r_p	3.14	2.82	3.01	2.56	3.47	3.20

Expt. #	63 / 3T3G	64 / 2T4G	65 / 2T4G	68 / 2T4G	69 / 2T4G	
$D_{b,O}$	8.0×10^{-14}	8.0×10^{-6}	2.4×10^{-11}	6.4×10^{-14}	9.6×10^{-15}	
$D_{b,T}$	$< 5.0 \times 10^{-14}$	5.0×10^{-6}	1.5×10^{-11}	$< 4.0 \times 10^{-14}$	$< 6.0 \times 10^{-15}$	
k_{SLR}	4.2×10^{-10}	2.0×10^{-10}	2.4×10^{-10}	2.4×10^{-10}	2.4×10^{-10}	
$[O_3]_g$	3.2×10^{14}	4.1×10^{14}	3.0×10^{14}	3.2×10^{14}	4.2×10^{14}	
$[STS]_{b,0}$	4.7×10^{21}	1.2×10^{21}	2.3×10^{21}	2.3×10^{21}	2.3×10^{21}	
$K_{sol,O3}$	3.4×10^{-9}	7.0×10^{-7}	2.2×10^{-8}	2.3×10^{-8}	1.3×10^{-8}	
r_p	3.08	4.43	3.04	2.99	3.38	

Table S4. Input parameters of KM-SUB simulations via Scenario 2 for the data of Expt. # listed below.

Expt. #	10 / 5T1S	26 / 4T2S	27 / 4T2S	28 / 4T2S	29 / 4T2S	30 / 4T2S
$D_{b,O}$	7.3×10^{-11}	8.0×10^{-11}	6.4×10^{-11}	7.2×10^{-11}	1.9×10^{-11}	1.3×10^{-11}
$D_{b,T,fast}$	4.6×10^{-11}	5.0×10^{-11}	4.0×10^{-11}	4.5×10^{-11}	1.2×10^{-11}	8.0×10^{-12}
$D_{b,T,slow}$	$< 5.0 \times 10^{-14}$	$< 5.8 \times 10^{-14}$	3.0×10^{-14}	$< 2.0 \times 10^{-14}$	$< 9.0 \times 10^{-15}$	$< 2.5 \times 10^{-14}$
k_{SLR}	3.8×10^{-10}	3.5×10^{-10}	3.7×10^{-10}	3.4×10^{-10}	4.0×10^{-10}	4.1×10^{-10}
$[O_3]_g$	3.6×10^{14}	4.0×10^{14}	3.6×10^{14}	4.0×10^{14}	3.6×10^{14}	3.8×10^{14}
$[STS]_{b,0}$	4.4×10^{21}	3.9×10^{21}	4.2×10^{21}	3.9×10^{21}	4.4×10^{21}	4.7×10^{21}
$[STS]_{b,0,fast}$	3.2×10^{21}	1.6×10^{21}	2.8×10^{21}	1.7×10^{21}	4.4×10^{20}	5.7×10^{20}
$K_{sol,O3}$	2.4×10^{-8}	2.8×10^{-8}	1.5×10^{-8}	2.7×10^{-8}	9.6×10^{-9}	8.8×10^{-9}
r_p	2.58	2.95	2.71	3.08	3.14	2.71

Expt. #	35 / 3T3S	36 / 3T3S	48 / 5T1G	49 / 5T1G	55 / 4T2G	56 / 4T2S
$D_{b,O}$	4.8×10^{-10}	1.0×10^{-10}	8.0×10^{-11}	1.1×10^{-10}	1.6×10^{-10}	7.2×10^{-12}
$D_{b,T,fast}$	3.0×10^{-10}	6.5×10^{-11}	5.0×10^{-11}	7.0×10^{-11}	9.8×10^{-11}	4.0×10^{-12}
$D_{b,T,slow}$	$< 1.8 \times 10^{-13}$	$< 2.8 \times 10^{-13}$	$< 1.5 \times 10^{-14}$	$< 5.0 \times 10^{-15}$	$< 2.0 \times 10^{-14}$	$< 1.0 \times 10^{-13}$
k_{SLR}	2.5×10^{-10}	2.5×10^{-10}	4.7×10^{-10}	6.6×10^{-10}	5.6×10^{-10}	5.3×10^{-10}
$[O_3]_g$	3.2×10^{14}	3.4×10^{14}	3.0×10^{14}	3.6×10^{14}	4.8×10^{14}	3.8×10^{14}
$[STS]_{b,0}$	2.2×10^{21}	2.5×10^{21}	5.3×10^{21}	6.7×10^{21}	6.0×10^{21}	5.5×10^{21}
$[STS]_{b,0,fast}$	1.1×10^{21}	1.7×10^{21}	3.5×10^{21}	2.2×10^{21}	2.6×10^{21}	3.9×10^{21}
$K_{sol,O3}$	1.4×10^{-7}	1.4×10^{-7}	5.3×10^{-9}	7.44×10^{-10}	4.7×10^{-10}	3.5×10^{-10}
r_p	2.95	3.01	2.94	3.08	3.14	2.77

Expt. #	60 / 3T3G	61 / 3T3G	66 / 2T4G	67 / 2T4G		
$D_{b,O}$	3.2×10^{-11}	3.2×10^{-11}	1.6×10^{-11}	1.1×10^{-10}		
$D_{b,T,fast}$	2.0×10^{-11}	2.0×10^{-11}	1.0×10^{-11}	7.0×10^{-11}		
$D_{b,T,slow}$	$< 1.0 \times 10^{-13}$	$< 3.0 \times 10^{-13}$	$< 3.0 \times 10^{-13}$	$< 5.0 \times 10^{-15}$		
k_{SLR}	3.3×10^{-10}	3.7×10^{-10}	2.5×10^{-10}	2.4×10^{-10}		
$[O_3]_g$	3.0×10^{14}	3.0×10^{14}	4.0×10^{14}	4.1×10^{14}		
$[STS]_{b,0}$	3.7×10^{21}	4.2×10^{21}	2.5×10^{21}	2.3×10^{21}		
$[STS]_{b,0,fast}$	7.0×10^{20}	8.4×10^{20}	1.1×10^{21}	1.3×10^{21}		
$K_{sol,O3}$	1.6×10^{-8}	5.1×10^{-9}	1.4×10^{-8}	2.2×10^{-8}		
r_p	3.05	3.32	2.94	3.14		

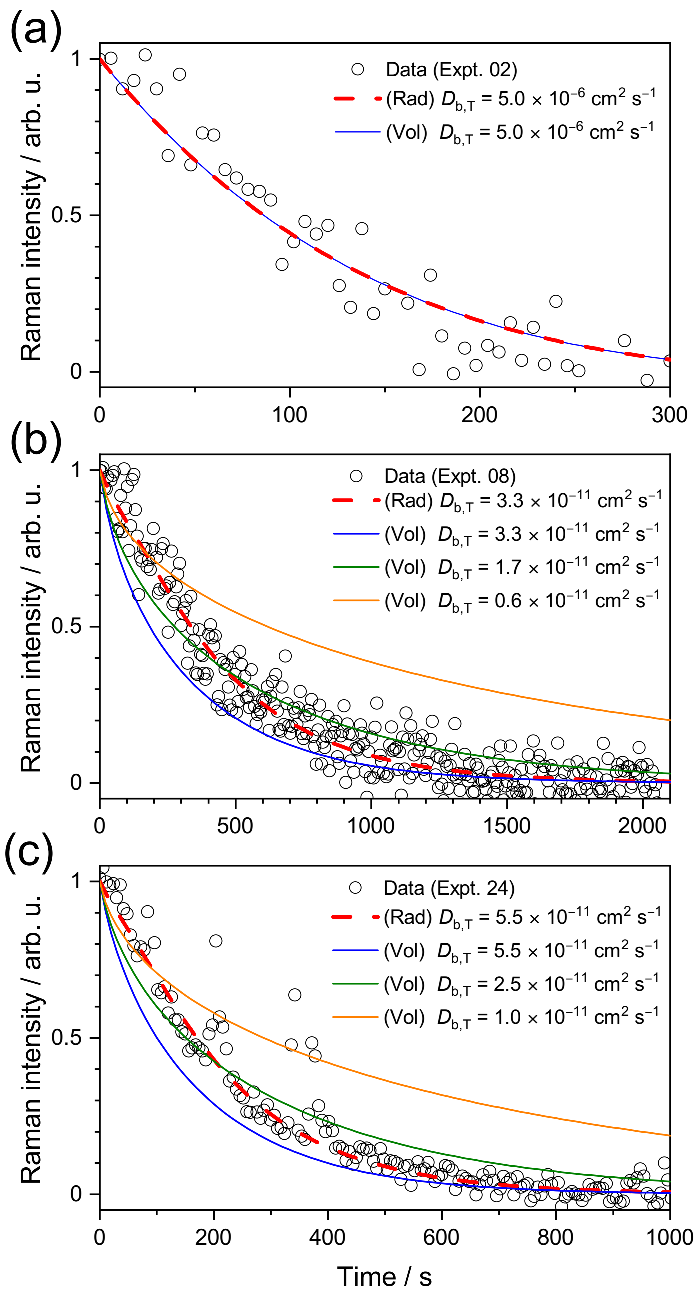

Fig. S3 (a) Symbols: kinetic measurement results of ternary STS:sucrose 5:1 mass ratio at 83% RH (Expt. 02). Dashed and solid lines: radial-averaged and volume-averaged simulation results of KM-SUB model utilizing the input parameters of Expt. 02 in Table S3, respectively. (b) Symbols: kinetic measurement results of ternary STS:sucrose 5:1 mass ratio at 40% RH (Expt. 08). Dashed line: radial-averaged simulation results of KM-SUB model utilizing the input parameters of Expt. 08 in Table S3. Solid lines: volume-averaged simulation results of KM-SUB model utilizing the input parameters of Expt. 08 in Table S3 while also adapting different values of $D_{b,T}$. (c) Symbols: kinetic measurement results of ternary STS:sucrose 4:2 mass ratio at 42% RH (Expt. 24). Dashed line: radial-averaged simulation results of KM-SUB model utilizing the input parameters of Expt. 24 in Table S3. Solid lines: volume-averaged simulation results of KM-SUB model utilizing the input parameters of Expt. 24 in Table S3 while also adapting different values of $D_{b,T}$.

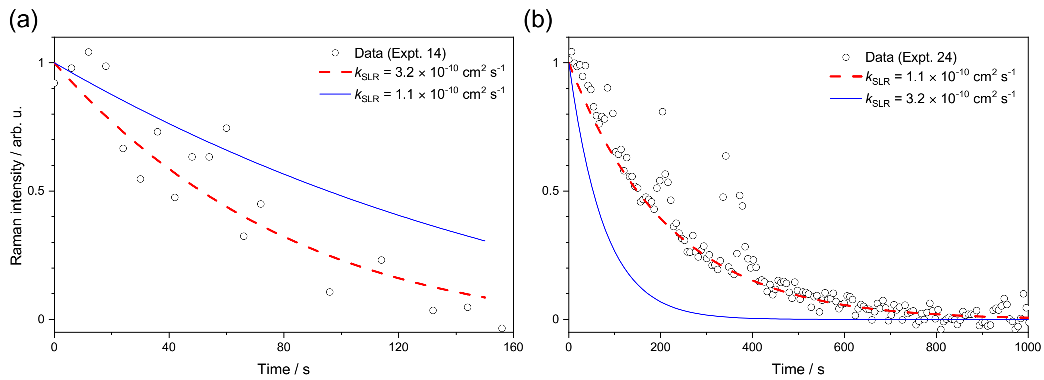

Fig. S4 (a) Symbols: kinetic measurement results of ternary STS:sucrose 4:2 mass ratio at 89% RH (Expt. 14). Dashed and solid lines: KM-SUB simulation results utilizing $k_{SLR} = 3.2 \times 10^{-10}$ cm^{2}s^{-1} and 1.1×10^{-10} cm^{2}s^{-1}, respectively. The value of $D_{b,T}$ is fixed to 1×10^{-5} cm^2 s^{-1}. Except k_{SLR} and $D_{b,T}$, the rest input parameters are the same as those for Expt. 14 in Table S3. (b) Symbols: kinetic measurement results of ternary STS:sucrose 4:2 mass ratio at 42% RH (Expt. 24). Dashed and solid lines: KM-SUB simulation results utilizing $k_{SLR} = 1.1 \times 10^{-10}$ cm^{2}s^{-1} and 3.2×10^{-10} cm^{2}s^{-1}, respectively. The value of $D_{b,T}$ is fixed to 1×10^{-5} cm^{2}s^{-1}. Except k_{SLR} and $D_{b,T}$, the rest input parameters are the same as those for Expt. 24 in Table S3.

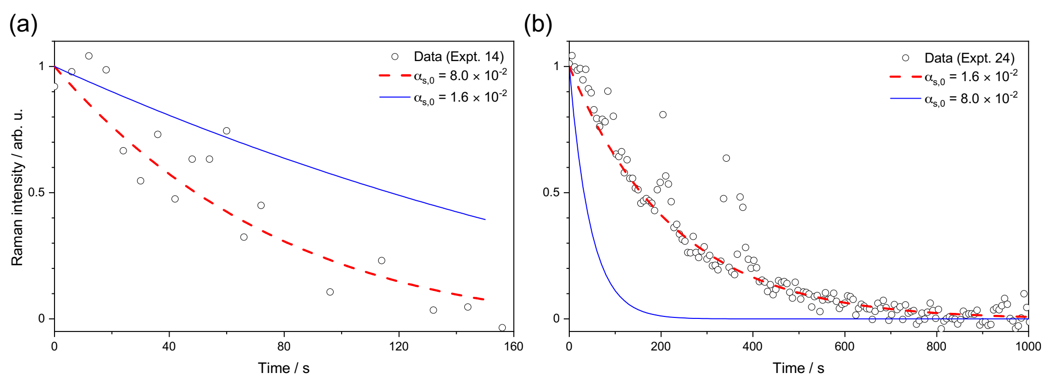

Fig. S5 (a) Symbols: kinetic measurement results of ternary STS:sucrose 4:2 mass ratio at 89% RH (Expt. 14). Dashed and solid lines: KM-SUB simulation results utilizing $\alpha_{s,0} = 8.0 \times 10^{-2}$ and 1.6×10^{-2}, respectively. The value of $D_{b,T}$ is fixed to 1×10^{-5} cm^2 s^{-1}. Except $\alpha_{s,0}$ and $D_{b,T}$, the rest input parameters are the same as those for Expt. 14 in Table S3. (b) Symbols: kinetic measurement results of ternary STS:sucrose 4:2 mass ratio at 42% RH (Expt. 24). Dashed and solid lines: KM-SUB simulation results utilizing $\alpha_{s,0} = 1.6 \times 10^{-2}$ and 8.0×10^{-2}, respectively. The value of $D_{b,T}$ is fixed to 1×10^{-5} cm^{2}s^{-1}. Except $\alpha_{s,0}$ and $D_{b,T}$, the rest input parameters are the same as those for Expt. 24 in Table S3.

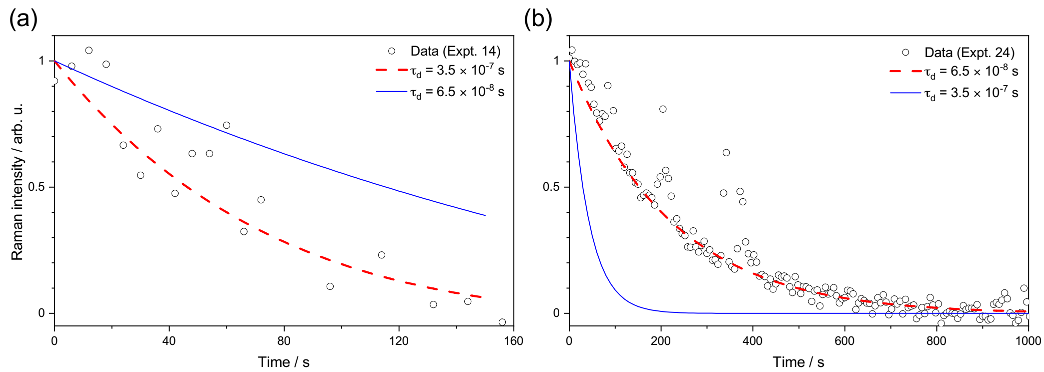

Fig. S5 (a) Symbols: kinetic measurement results of ternary STS:sucrose 4:2 mass ratio at 89% RH (Expt. 14). Dashed and solid lines: KM-SUB simulation results utilizing τ_d = 3.5×10^{-7} s and 6.5×10^{-8} s, respectively. The value of $D_{b,T}$ is fixed to 1×10^{-5} cm^2 s^{-1}. Except τ_d and $D_{b,T}$, the rest input parameters are the same as those for Expt. 14 in Table S3. (b) Symbols: kinetic measurement results of ternary STS:sucrose 4:2 mass ratio at 42% RH (Expt. 24). Dashed and solid lines: KM-SUB simulation results utilizing τ_d = 6.5×10^{-8} s and 3.5×10^{-7} s, respectively. The value of $D_{b,T}$ is fixed to 1×10^{-5} cm^{2}s^{-1}. Except τ_d and $D_{b,T}$, the rest input parameters are the same as those for Expt. 24 in Table S3.

III. CERS characterization

Table S5. Spectral positions of CERS assigned from the data of Expt. 10, 12 and 59 (see Table S1) and the corresponding simulation results of *mrfit*.

Data: Expt. No. 10
Reaction time (second): 0
Radius (μm): 3.050
m0: 1.535
m1 (nm): 20.570
Mean error squared -- Wavelength^2: 8.4811372954842167E-003

λ(Obs.) (nm)	λ(Calc.) (nm)	Mode order	Mode number	Polarization
553.92	554.03	2	42	TE
555.07	554.93	1	47	TE
565.25	565.35	2	41	TE
565.90	565.84	1	46	TE
570.18	570.13	2	40	TM
577.11	577.16	2	40	TE
627.86	627.90	1	41	TE
630.12	630.20	2	36	TE
632.46	632.33	1	40	TM

Data: Expt. No. 12
Reaction time (second): 0
Radius (μm): 2.751
m_0: 1.547
m_1 (nm): 23.368
Mean error squared -- Wavelength^2: 3.4829961369253872E-003

λ(Obs.) (nm)	λ(Calc.) (nm)	Mode order	Mode number	Polarization
631.98	631.92	1	36	TM
627.05	627.03	1	37	TE
560.87	560.96	2	37	TE
566.28	566.32	2	36	TM
573.80	573.83	2	36	TE
559.58	559.59	1	42	TE
563.37	563.30	1	41	TM
571.86	571.84	1	41	TE
575.74	575.75	1	40	TM
579.46	579.56	2	35	TM
584.71	584.67	1	40	TE
587.37	587.34	2	35	TE
598.04	598.11	1	39	TE
612.18	612.21	1	38	TE
616.54	616.51	2	33	TE
553.84	553.71	2	37	TM
623.66	623.66	2	32	TM

Data: Expt. No. 59
Reaction time (second): 1020 (The reaction completes.)
Radius (μm): 3.306
m_0: 1.424
m_1 (nm): 14.282
Mean error squared -- Wavelength^2: 9.5320458065408528E-004

λ(Obs.) (nm)	λ(Calc.) (nm)	Mode order	Mode number	Polarization
541.90	541.84	1	49	TM
547.20	547.18	1	44	TE
548.22	548.21	1	49	TE
552.05	552.03	1	48	TM
558.63	558.63	1	48	TE
562.60	562.63	1	47	TM
569.40	569.47	1	47	TE
573.60	573.66	1	46	TM
580.75	580.75	1	46	TE
585.10	585.14	1	45	TM
592.50	592.51	1	45	TE
597.10	597.12	1	44	TM
604.80	604.78	1	44	TE
609.65	609.61	1	43	TM
617.65	617.58	1	43	TE

Data: Expt. No. 59 Reaction time (second): 0 (prior reaction) Radius (μm): 3.360 m_0: 1.428 m_1 (nm): 15.953 Mean error squared -- Wavelength^2: 2.9218372320652742E-003				
λ(Obs.) (nm)	λ(Calc.) (nm)	Mode order	Mode number	Polarization
542.10	542.04	1	48	TM
547.90	547.90	1	43	TE
548.52	548.50	1	48	TE
552.45	552.46	1	47	TM
559.13	559.16	1	47	TE
563.30	563.31	1	46	TM
570.25	570.26	1	46	TE
574.60	574.61	1	45	TM
581.80	581.83	1	45	TE
586.35	586.39	1	44	TM
598.65	598.68	1	43	TM
606.50	606.49	1	43	TE
611.55	611.52	1	42	TM
619.70	619.64	1	42	TE

In the simulations of MRFIT,[1] the range of possible mode orders defined in the present work is from 1 to 2. The value of droplet RI (m) is assumed to have a monotonic dependence with CERS wavelengths (λ), i.e., $m = m_0 + m_1(1/\lambda - 1/\lambda_0)$, where the midpoint λ_0 is set to 589.3 nm. The RI of air was fixed to 1. Table S5 shows the representative assignments of CERs spectral positions and simulated radius, m_0 and m_1 from the simulation results of *mrfit*.

IV. Effect of solute strength on Henry's law constant

Here we followed the methodology utilized by Weisenberger and Schumpe[2] to estimate the Henry's law coefficient of ozone in salt solutions, H_S, with Sechenov constants of ion i, K_i:

$$\log\left(\frac{H}{H_s}\right) = \sum_i K_i[i] = \sum_i (h_i + h_{O3})[i] \qquad \text{(S1)}$$

where H is the Henry's law coefficient of ozone in pure water, h_i, is an ion-specific parameter, h_{O3} is an ozone-specific parameter, and $[i]$ is the concentration of ion i. The values of h_i for i = Na^+ and $S_2O_3^{2-}$ measured by Weisenberger and Schumpe are 0.1143 m^3/kmol and 0.1270 m^3/kmol, respectively.[2] The expression for the Sechenov constant of ozone, h_{O3}, is assumed to be a linear function of the temperature T:

$$h_{O3} = h_{O3,0} + h_T(T - 298.15\text{K}) \quad \text{(S2)}$$

with $h_{O3,0}$ = 0.00396 m^3/kmol and h_T = 0.00179 m^3/(kmol•K).[3] The temperature in this study is 298 K. The standard deviation of these Sechenov constants is 0.026.[2]

For the case of the aqueous solution containing nonelectrolytes, such as glucose and sucrose, the corresponding Sechenov constant K_n can be expressed as:[4]

$$K_n = b_n + b_{O3,0} + b_{O3,T}(T - 298.15\text{K}) \quad \text{(S3)}$$

The values of b_n for glucose and sucrose are 6.68 $\times$ 10^{-4} m^3 kg^{-1} and 5.85 $\times$ 10^{-4} m^3 kg^{-1}, respectively.[4] Finally, as we cannot find any literature value of $b_{O3,0}$ and $b_{O3,T}$, we used those for O_2 instead: $b_{O2,0}$ = 0 m^3 kg^{-1} and $b_{O2,T}$ = -0.044×10^{-4} m^3/(kmol•K).[4] Bin suggested that the values suggested for oxygen are applicable in ozone systems.[5]

V. Error analysis

The methodology for error propagations is similar to our previous works.[6, 7] The percentage error of each solute concentration, such as $[\text{STS}]_0$, $[\text{glucose}]_0$ and $[\text{sucrose}]_0$, reported in Tables S1-S2 is 2.6% on average, which is attributed to fitting error of calibration curves and statistic error of aerosol Raman spectroscopy measurements. The deviation of each Henry's Law constant is estimated from the errors of solute concentrations. The error bar of each droplet radius reported in Tables S1-S2 is assumed to be 0.15 μm, which is an averaged change of the radius during the reaction progress. The percentage error of each ionic strength I in Tables S1-S2 is 12% on average, which is contributed by the errors of solute concentrations and the change of the droplet volume during the reaction progress. The percentage error of the ozone pressure is 2.6%, which is the assumed maximum error of the measured UV absorption cross section of ozone at 250 nm estimated by literature.[8] The error of each fitted D reported Figs. 3 and 5 are attributed to fitting errors.

V. Partial depletion in the case of binary STS-water system

In our previous study, i.e., Hsu et al.,[7] the kinetic data of Expt. 16−19 also exhibit the feature of partial depletion, and Table S6 list the values of ϕ_{fast} of these data, as well as their experimental conditions. It should note that the fitted values of k_{SLR} for these data remain the same as those in Hsu et al.,[7] and thus the empirical relationship of k_{SLR} listed in Table 1 of the main text remains the same as that provided by Hsu et al.[7] It should note that according to Table S6, ϕ_{fast} starts to decrease when increasing [STS], after [STS] is larger than 10 M. The spectral drifts of $\nu_{sym(\mathrm{S-O})}$ Raman band of Expt. 16–19 indicates that STS is in the state of supersaturation but no crystallization. Thus, we conclude that the decrease of ϕ_{fast} is not due to phase transition to solid phase, and the effect leading to this decrease of ϕ_{fast} should depend on [STS]. However, it should also note that [STS] of binary STS-water system associated with $\phi_{\mathrm{fast}} < 1$ is around 13-20 M, while that for ternary STS-sucrose/glucose-water system associated with $\phi_{\mathrm{fast}} < 1$ is significantly smaller 10 M in general, indicating the potential role of organics, i.e., sucrose and glucose.

Table S6. RH, ϕ_{fast}, $[\mathrm{STS}]_{\mathrm{b,0}}$ and Raman shift of $\nu_{sym(\mathrm{S-O})}$ of Expt. 16–19 in Hsu et al.[7]

Expt. #	RH (%)	ϕ_{fast}	$[\mathrm{STS}]_{\mathrm{b,0}}$ (M)	$\nu_{sym(\mathrm{S-O})}$ (cm^{-1})
1–13	85–71	1.0	2.8–5.9	996.9–998.3
14	61	1.0	10.1	1004.0
15	61	1.0	10.0	1004.0
16	33	0.6	12.7	1011.2
17	33	0.5	16.1	1011.2
18	32	0.5	19.8	1011.2
19	29	0.3	17.1	1011.2

References

1. T. C. Preston and J. P. Reid, *J. Opt. Soc. Am. A*, 2015, **32**, 2210.
2. S. Weisenberger and A. Schumpe, *AIChE Journal*, 1996, **42**, 298-300.
3. E. Rischbieter, H. Stein and A. Schumpe, *Journal of Chemical & Engineering Data*, 2000, **45**, 338-340.
4. E. Rischbieter, A. Schumpe and V. Wunder, *Journal of Chemical & Engineering Data*, 1996, **41**, 809-812.
5. A. K. Biń, *Ozone: Science & Engineering*, 2006, **28**, 67-75.
6. Y. P. Chang, S. J. Wu, M. S. Lin, C. Y. Chiang and G. G. Huang, *Phys. Chem. Chem.*

Phys., 2021, **23**, 10108 - 10117.

7. S.-H. Hsu, F.-Y. Lin, G. G. Huang and Y.-P. Chang, *J. Phy. Chem. C*, 2023, **127**, 6248-6261.

8. J. P. Burrows, A. Richter, A. Dehn, B. Deters, S. Himmelmann, S. Voigt and J. Orphal, *Journal of Quantitative Spectroscopy and Radiative Transfer*, 1999, **61**, 509-517.